Ewing Sarcoma

Pream Kadevari; Richard B. Towbin; MD, Carrie M. Schaefer, MD; Alexander J. Towbin, MD

Case Summary

A teenager presented with a three-week history of right-sided headaches, double vision, intermittent somnolence, and left lower extremity stinging pain and weakness. Additionally, there was left lower extremity weakness on physical examination. The initial imaging included MRI of the brain and spine. A percutaneous biopsy of the posterior right parietal superficial mass was performed, with a pathologic diagnosis of Ewing Sarcoma (EWS). The primary lesion was later confirmed to arise from the left fibula (not shown) on radiographs, PET/CT and MRI where the soft tissue component was best seen.

Imaging Findings

Brain MRI (Figure 1) demonstrated diffuse calvarial signal abnormality and multiple bilateral epidural and scalp masses, the largest overlying the posterior right parietal bone.

Affiliations: Lincoln Memorial University, DeBusk College of Osteopathic Medicine (Mr Kadevari); Department of Radiology, Phoenix Children's Hospital (Drs Schaefer, R. Towbin); Cincinnati Children's Hospital and University of Cincinnati College of Medicine (Dr A. Towbin)

Spine MRI (Figure 2) demonstrated multiple abnormally contrast-enhancing vertebral bodies and mild loss of height at T9 and T11.

Whole body FDG-PET and axial PET/CT through the thorax performed one year after diagnosis demonstrated multifocal FDG uptake in metastatic pleural-based masses, multiple vertebrae, and bilateral extremities.

Diagnosis

Metastatic Ewing sarcoma.

The differential diagnoses for EWS include osteomyelitis and osteosarcoma, both of which can have similar clinical presentations and appear similarly on imaging. Noteworthy imaging features of EWS may help distinguish EWS from these other common bone lesions. When comparing EWS to osteosarcoma, on radiography osteosarcoma typically has mixed lytic and sclerotic destructive bone changes with a periosteal reaction generally perpendicular to the diaphyseal cortex. In contrast, EWS is significantly more likely to show metadiaphyseal involvement.[1,2] Other noteworthy but not pathognomonic characteristics of EWS on radiography include an "onion-skinning" periosteal bone pattern, "hair on end" appearance, and cortical saucerization.[1,2]

Osteomyelitis may be best differentiated from EWS on MRI. EWS is significantly more likely to show heterogeneous cystic and necrotic areas with a contrast-enhancing soft tissue mass, a wide transition zone, and permeative cortical involvement.[1,2] EWS will not show the serpiginous tracks that may be appreciated in osteomyelitis.[2] When comparing the low signal intensity of altered bone on T1 to the hyperintense signal of normal marrow on STIR images, the margins between normal bone and affected regions tend to be more sharply defined in EWS when compared to osteomyelitis.[3]

Discussion

Ewing sarcoma is a malignant tumor of childhood that is described by a t(11;22)(q24;q12) translocation and "small round blue cells" on histology.[6] Ewing sarcoma has an annual incidence of one case per million in the United states with peak morbidity occurring between 15-18 years of age.[7] While similar in histological appearance, EWS is distinct from primitive neuroectodermal tumors, since these tumors lack the *MIC2* gene and do not

Figure 1. (A) Brain MRI axial T2 demonstrating diffuse osseous signal heterogeneity and multiple bilateral epidural and scalp masses, the largest overlying the posterior right parietal bone (arrow). The epidural component partially compressed the posterior aspect of the superior sagittal sinus. (B) Brain MRI axial T1 postcontrast with fat suppression demonstrating heterogeneously enhancing diffuse osseous lesions with epidural (*) and scalp extension (arrows). Areas without enhancement (blue star) reflect necrosis.

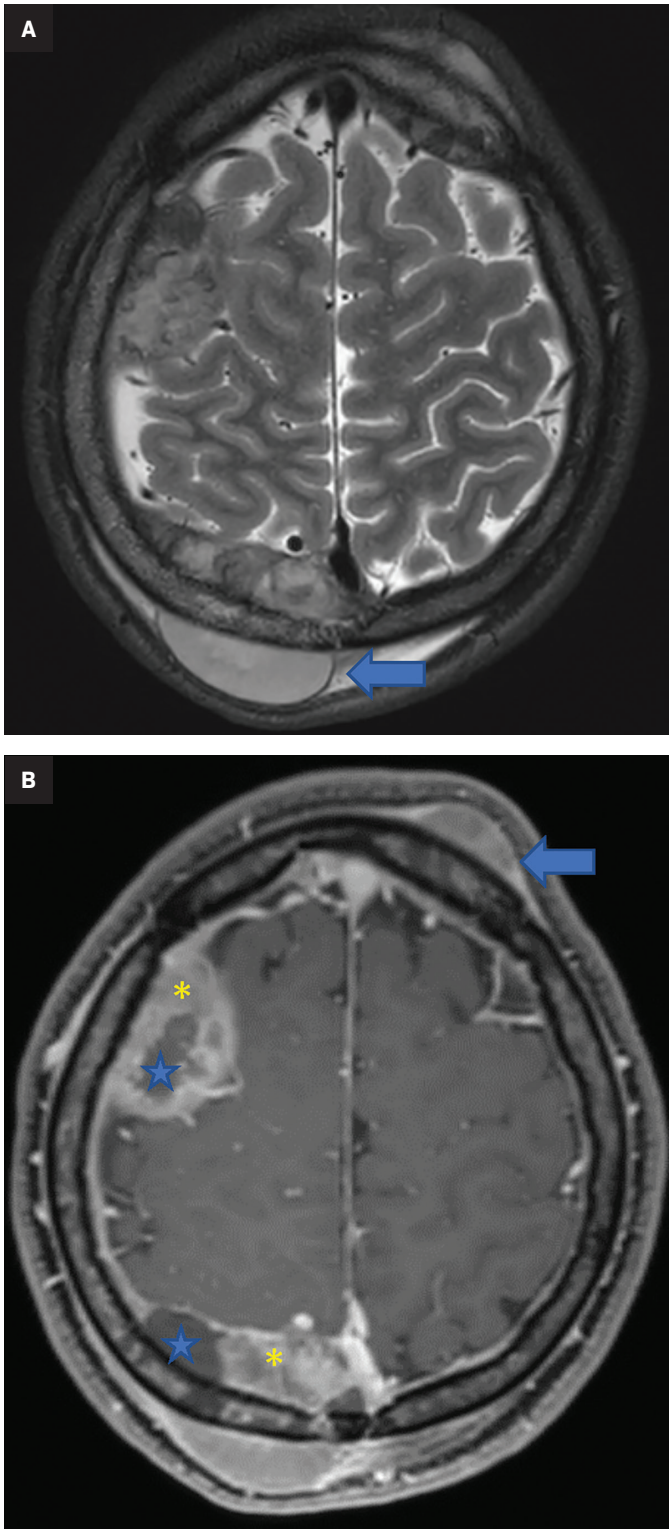

Figure 2. Spine MRI T1 postcontrast with fat suppression demonstrating multiple enhancing vertebral bodies with loss of height at the T9 and T11 levels (*).

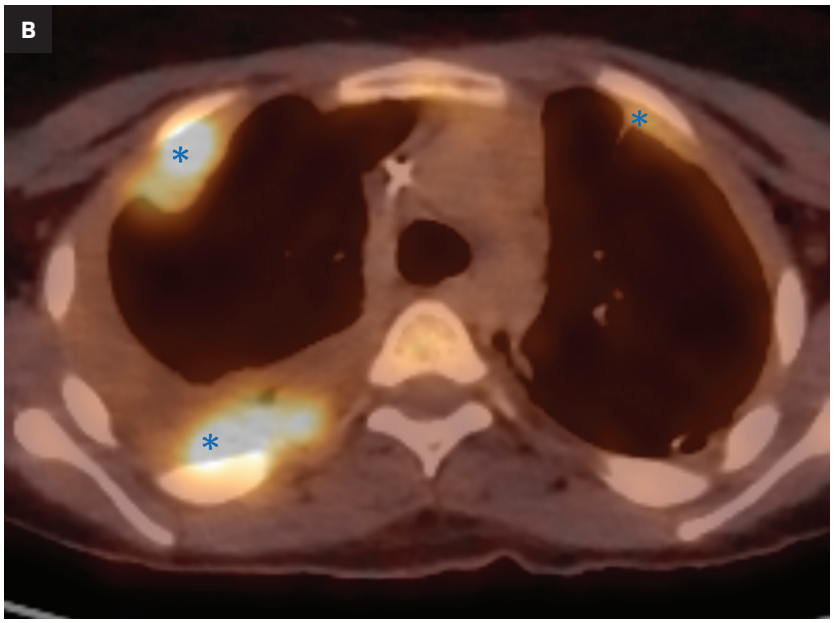

Figure 3. (A) Whole body FDG-PET and (B) axial PET/CT through thorax one year after diagnosis demonstrate multifocal FDG uptake in metastatic pleural-based masses (asterisks), multiple vertebrae, and bilateral extremities (arrows). Note the recurrent large soft tissue mass in the right lateral calf region.

express CD99.[4] Primary EWS most commonly arises in the diaphysis of long bones but may also present in the ribs, flat bones of the pelvis, and spinal column.[6] Distant metastasis most commonly occurs in the lungs (38%), spine (31%), and bone marrow (11%), with skull metastasis being the rarest presentation, occurring in only 2-9% of cases.[8,9]

Definitive diagnosis of EWS can be made with cytogenetic testing for the *EWSR1* gene, which acts as a transcription factor created by fusion of the *EWS* gene located on 22q12 and friend of leukemia virus integration 1 (*FLI1*) gene, located on 11q24, forming a t(11;22)(q24;q12) *EWS-FLI1* translocation.[4] Cell surface protein CD99, though highly sensitive for EWS, is a non-specific marker also seen in lymphoblastic lymphoma, rhabdomyosarcoma, and ependymoma.[4] The presence of other reported markers in combination with CD99, such as NKX2-2, a downstream target of *EWS-FLI1*, is highly specific for EWS.[5] These markers can aid in the differentiation of EWS from other closely related head and neck malignancies such as adamantinoma-like Ewing sarcoma that cannot be differentiated on imaging.[5]

Clinical features include non-specific constitutional signs and symptoms such as fever, anemia, fatigue, nausea, and vomiting.[6,8,9] In the case of calvarial involvement, local symptoms include headache and papilledema due to high intracranial pressures, ear drainage, facial muscle weakness and paralysis. An enlarging, often immobile, non-tender mass may be present on examination.[6,8,9] Lab values may reveal neutrophilia and leukocytosis.[6]

Radiographic features of EWS show bone destruction with an associated large soft tissue mass. The associated bone destruction has a multilayered "onion-skin" like pattern of new periosteal bone formation.[6] However, this finding is not usually appreciated on skull lesions and has otherwise been reported as a lytic mass with mottled bone destruction.[8] MRI findings of primary cranial EWS appear as hypointense on T1, and hypo- to hyperintense on T2.[9] Affected bone margins have very low signal intensity on T1 images, while normal bone has a high signal intensity on T2 or STIR images, which creates a sharply defined margin helping to distinguish EWS from other primary malignant bone tumors.[3]

For evaluation of the primary lesion and osseous metastasis, the

Children's Oncology Group recommends obtaining imaging studies both at time of presentation, at baseline once local control has been achieved, surveillance while on chemotherapy, and upon completion of the treatment regimen. Anterior-posterior and lateral radiographs as well as contrast-enhanced MRI or CT are often the initial imaging studies. Technetium-99m-methylene-diphosphonate bone scintigraphy or Fluorodeoxyglucose PET is the modality of choice for whole body evaluation.

Treatment for EWS involves chemotherapy in combination with radiotherapy. The standard chemotherapeutic protocol typically includes vincristine, doxorubicin, cyclophosphamide, ifosfamide and etoposide.[9] Radiotherapy may be used in combination with surgery, as warranted.[6]

Conclusions

Ewing sarcoma with skull metastasis is a rare occurrence. The aggressive nature of this tumor and poor prognosis in the case of skull metastasis makes early detection and treatment paramount.

Characteristic findings of EWS on plain radiograph can help in differentiating EWS from osteosarcoma, while MRI can aid in distinguishing EWS from osteomyelitis. Imaging is essential for locating the lesion(s), establishing a baseline, and monitoring for recurrence throughout and following the course of treatment. Definitive diagnosis of EWS can be made with cytogenetic testing.

References

1) Heare T, Hensley MA, Dell'Orfano S. Bone tumors: osteosarcoma and Ewing's sarcoma. *Curr Opin Pediatr*. 2009;21(3):365-372. doi:10.1097/MOP.0b013e32832b1111

2) McCarville MB, Chen JY, Coleman JL, et al. Distinguishing Osteomyelitis from Ewing sarcoma on radiography and MRI. *AJR Am J Roentgenol*. 2015;205(3):640-651. doi:10.2214/AJR.15.14341

3) Henninger B, Glodny B, Rudisch A, et al. Ewing sarcoma versus osteomyelitis: differential diagnosis with magnetic resonance imaging. *Skeletal Radiol.* 2013;42(8):1097-104. doi: https://doi.org/10.1007/s00256-013-1632-5

4) Yang MJ, Whelan R, Madden J, et al. Intracranial Ewing sarcoma: four pediatric examples. *Childs Nerv Syst*. 2018;34(3):441-448. doi:10.1007/s00381-017-3684-7

5) de Alva E, Marcilla D, Biscuola M. *Practical Soft Tissue Pathology: A Diagnostic Approach* (Second Edition). Elsevier, 2019. https://doi.org/10.1016/B978-0-323-49714-5.00008-9.

6) Ye C, Wei W, Tang X, et al. Sacral Ewing sarcoma with rib, lung, and multifocal skull metastases: A rare case report and review of treatments. *Front Oncol.* 2022;12:933579. Published 2022 Sep 8. doi:10.3389/fonc.2022.933579

7) Khan S, Abid Z, Haider G, et al. Incidence of Ewing's sarcoma in different age groups, Their associated features, and its correlation with primary care interval. *Cureus.* 2021;13(3): e13986. doi:10.7759/cureus.13986

8) Rana K, Wadhwa V, Bhargava EK, Batra V, Mandal S. Ewing's sarcoma multifocal metastases to temporal and occipital bone: A rare presentation. *J Clin Diagn Res.* 2015;9(6):MD04-MD5. doi:10.7860/JCDR/2015/13254.6071

9) Moschovi M, Alexiou GA, Tourkantoni N, et al. Cranial Ewing's sarcoma in children. *Neurol Sci*. 2011;32(4):691-694. doi:10.1007/s10072-011-0509-4